

# Cloud-based Rainfall-run-off Model for Assessment of Long-Term Rainfall Variability and Trends Using Google Earth Engine

D. Vetrithangam<sup>1\*</sup>, B. Arunadevi<sup>2</sup>,  
Naresh Kumar Pegada<sup>3</sup>, Sukhpreet Kaur<sup>4</sup>, B. Krishna Prasad<sup>5</sup>

<sup>1</sup>Department of Computer Science & Engineering, Chandigarh University, Mohali, 140413, India

<sup>2</sup>Department of ECE, Dr. N.G.P Institute of Technology, Coimbatore, India

<sup>3</sup>Department of CSE (AI & ML), Keshav Memorial Engineering College, Telangana, India

<sup>4</sup>Department of Computer Science & Engineering, Chandigarh University, Mohali, 140413, India

<sup>5</sup>Department of CSE, Koneru Lakshmaiah Education Foundation, Vaddeswaram, Guntur, Andhra Pradesh, India.

Received on 31 August 2023; Accepted on 27 November 2024

## Abstract

Several engineering constructions, such as canals, bridges, culverts, and road drainage systems, depend on rainfall for their creation. Different types of rainfalls normal, deficit, excessive, and seasonal are all understood using the daily rainfall data for the seven-year timeframe (2015–2021). Farmers, urban engineers, and planners of water resources will all benefit from the knowledge provided by this analysis as they determine the availability of water and plan the appropriate storage. To examine the variability in rainfall, the average, total monthly and annual rainfalls were determined. Most existing techniques used the curve number method to compute statistical rainfall runoff for a particular region; this technique ignores the effects of rain intensity and duration because it lacks an expression for time. The Soil Conservation Service curve number method is adaptable and widely used for runoff estimation. The main scope of this paper is to compute the statistical analysis of rainfall-runoff for the state of Andhra Pradesh. The SCS-CN method is implemented in Google Earth Engine (GEE) on the satellite images to estimate the runoff for the state of Andhra Pradesh. The result demonstrates that the average and total runoff values from 2015 to 2021 are 151.1786, and 1058.25, respectively, and their average and total precipitation values are 926.5884 and 6486.119. And this research work finds the facts: the year 2020 has the highest rainfall (1276.32 mm); the year 2016 has the lowest runoff (591.33). Engineers and farmers will be able to determine the necessary input value for the design and analysis of engineering constructions as well as for crop planning with the assistance of the computed detailed statistical analysis of this region.

© 2025 Jordan Journal of Earth and Environmental Sciences. All rights reserved

**Keywords:** Runoff, Precipitation, Curve Number, Land Cover, Land Use, Soil Texture, Google Earth Engine.

## 1. Introduction

Water is indispensable to all life processes and cannot be replaced. In addition to being a source of power and beneficial resource consumption within the country, agriculture, and industry, water is also important in transportation. Rainfall is a region's primary source of water, and it has a significant impact on agriculture. Plants obtain water from both natural sources and irrigation. Forecasting the likelihood of rainfall is crucial because crop production, especially in rain-fed areas, depends on rainfall patterns that can be analyzed using historical hydrological data and statistical methods. Probability distribution or occurrence aids in connecting the size of extreme occurrences such as flooding, droughts, and violent storms with the amount of times they occur, so that the likelihood of occurrence over time can be predictably calculated. The collection of hydrological data can be fitted with a frequency distribution to determine the likelihood that a random parameter will occur. To match the distribution, statistical parameters are employed to assess the hydrological data and evaluate its variability. For planning water resources, a number of models, ranging from conceptual to empirical

and physically based, have been developed. The most crucial hydrological component is run-off. The establishment of soil conservation procedures for projects was delegated to the Soil Conservation Services (SCS), which was established in 1933 (Abdul Ghani et al., 2016). Waterways, irrigation schemes, water harvesting, erosion control structures, and groundwater development strategies requires accurate estimation of surface runoff. However, hydrologists in Saudi Arabia face serious challenges, specifically due to the rare availability of surface runoff data. In this study, the soil conservation service-curve number (SCS-CN). In order to simulate the runoff process, the data-driven models identify the ideal correlation between the data inputs and the result series. In order to explain variations in runoff modeling and flood prediction, the benefits and drawbacks of the models above were finally explored (Ahmad et al., 2022). To estimate the surface run-off, Ahmad recommended taking into account factors such as soil, antecedent rainfall, geographical distribution, and land use/land cover (LULC) type. This classification represents a significant accomplishment for the SCS curve number (CN) method, which provides an

\* Corresponding author e-mail: vetrigold@gmail.com

observational connection to estimate run-off and considers initial abstraction, depending on the soil variety and LULC (Al-Ghobari et al. 2020). The CN approach is also used to calculate surface run-off by several of the popular models, like SWAT and HEC-HMS (Anderson et al., 2004; Gholami and Khaleghi, 2021). The SCS model was initially created for the USA to calculate the actual surface water runoff from tiny basins' few rainfalls (Animashaun et al., 2020) which is of prime importance in hydrological engineering, agricultural planning and management, environmental impact assessment, flood forecasting, and others fields. This article reviews the methodology and associated hydrological models used for runoff estimation along with their advantages and limitations. Furthermore, discussion focuses on the potential applications of Remote Sensing (RS, Arnold and Allen, 1996, Arvind et al., 2017).

The incident in December 2014 is one example of how an unforeseen heavy rainfall storm contributed to rainfall totals those broke records. Many of its occurrences are proof of global warming and climate change, which will have an impact on these extreme rainfall events (Baquero et al., 2005). In the past, highly accurate classical rain gauges or wide-area microwave radars have been used to confirm rainfall measurements. Rainfall occurrences' drop size distribution (DSD) must be investigated in order to create and validate more precise rainfall forecast algorithms. The dispersion of drop sizes will be investigated and used in the analysis of rain acquisition with a disdrometer, utilizing observations from the NASA TRMM satellite and rain gauges (Baquero et al., 2005). Rapid development over the past few decades has significantly altered the LULC pattern, which affects CN and hydrological factors affecting catchment run-off. Geospatial technology advancements make it easier to incorporate these elements when spatially and temporally estimating run-off. The utilization of digital elevation models for hydrological modeling depending on an area's topography has been made possible by the application of GIS (Soulis and Dercas, 2007). The soil composition, drains, LULC, geography parameters, and other region features can be extracted using RS and stored as a georeferenced database in a GIS. In the GIS context, the retrieved layers are then integrated with meteorological information for further analysis, interpretation, and visualization of evolving rainfall-runoff models (Chormanski et al., 2008, Sayd and Mubi, 2020). Employing a high-quality land surface model, such as a Digital Elevation Model (DEM), alongside data from Earth observation satellites' visual and radar systems is essential for identifying flood-prone regions and analyzing the impacts of flood events. This integrated approach enhances the understanding of flood dynamics and facilitates more effective flood management strategies (Ebrahimian et al., 2009). In order to categorize and analyze watershed areas and runoff models, remote sensing methods can supply data about the land surface's space and time. In order to confirm the results of spatial models, they can measure surface characteristics (like surface hardness, LULC class, etc.) and their time-based variations on the one hand and relate geologically significant areal phenomena on the other (Eliza et al., 2016, Gupta and J. Dixit, 2022).

According to the current statistical study, which offers a clear picture of rainfall data, the region does not have enough rainfall to support wet crop production. Improved irrigation and crop production in this region depend on the coordinated use of groundwater and accessible rainfall. The Soil Conservation Service Curve Number (SCS-CN) method is a widely used hydrological model for estimating direct runoff or infiltration from rainfall. Developed by the USDA's Soil Conservation Service, this method relies on a curve number (CN) that reflects land use, soil type, and antecedent moisture conditions (Soulis and Valiantzas, 2012, Soulis and Valiantzas, 2009).

The synergistic approach of remote sensing and GIS techniques enables efficient flash-flood monitoring and damage assessment in the Thessaly plain area. This integration enhances the accuracy of flood prediction and provides valuable insights for disaster management and mitigation strategies (Psomiadis et al., 2019). Empirical data from typhoon occurrences was used to test the correctness of the surface runoff model (Psomiadis et al., 2020). For a few specific rainfall occurrences in the watershed, the runoff depth was calculated using the NRCS-curve number approach (Rajbanshi, 2016.) A revisit of NRCS-CN Inspired Models coupled with RS and GIS for Runoff Estimation examines enhanced runoff estimation by integrating the NRCS-CN model with remote sensing (RS) and GIS. This approach improves spatial accuracy by using satellite data to capture land use, soil, and rainfall variability (Verma et al., 2017). Rainfall-Runoff Risk characteristics of Urban Function Zones in Beijing Using the SCS-CN Model examines runoff risks across various urban zones in Beijing. The SCS-CN model is applied to assess how land use and soil types influence runoff potential, supporting targeted flood management strategies for diverse urban functions (Wei et al., 2018).

The application of the NRCS-CN method enhances watershed runoff estimation and disaster risk assessment by using land and soil data to predict runoff levels. Integrating geomatics tools with this method improves accuracy in assessing natural hazards. This approach aids in disaster preparedness and risk management (Zhang, 2019). Research on Rainfall Estimation Based on Improved Techniques explores advancements in methods for more accurate rainfall estimation. The improved approach enhances the integration of real-time data, leading to better rainfall predictions (Zhang et al., 2022).

The SCS-CN approach was a useful tool in this study since it made it easy but effective to determine the direct runoff reaction for each soil, land usage, and maintenance combination (Jehanzaib et al., 2022). It incorporates several of the parameters of soil, land utilization, and land maintenance factors that have an impact on runoff generation into a single CN factor and includes simple-to-obtain and well-documented environmental inputs (Ling et al., 2020, Attah et al., 2020). Studies on rainfall variability used the linear regression model (LRM), precipitation concentration index, and rainfall variability index. Nonparametric Mann-Kendall (MK) tests and the Kriging interpolation method were

utilized for trend analysis and change point identification, as well as for the spatial analysis of rainfall (Salahat and Al-Qinna, 2015). Hypothetical probability distributions for initial loss data were evaluated for their influence on design flood estimates. The Beta and Gamma distributions effectively approximate initial losses in Australia. Sample size significantly impacts the accuracy of probability distributions, with mixed results observed based on varying thresholds (Loveridge and Rahman, 2021). To examine the rainfall-runoff stake features of the research field, the SCS-CN model was used. High runoff risk cluster locations were primarily found in the study area's centre, while areas with a low likelihood of runoff were mostly found among the roads. The two CN system approach outperforms earlier methods focused on a completely asymptotic CN value determination and offers reasonable accuracy (Psomiadis et al., 2020). The observed CN value fluctuation cannot always be explained by CN value variation based solely on AMC group (Moglen et al., 2022). The major goal of the 7KH model is to offer a useful tool in regions with severe fresh water shortages, growing water needs, and a severe lack of hydrometric data (Musgrave., 1955). Rainfall data was acquired from a global weather station using the Thiessen polygon method, which is related to a Geographic Information System application. The findings indicated that two rainfall stations described the rainfall variation across the study object (Nganro et al., 2020).

Measuring rainfall runoff can be a challenging task due to various factors that can affect the accuracy of measurements. It presents several challenges. First, inadequate instrumentation can significantly impact accuracy; the quality and proper calibration of measurement devices are crucial, as some instruments may lack sensitivity to low flows or may become clogged with debris. Additionally, land use changes, such as deforestation and urbanization, can alter the surface properties of a catchment, thereby affecting its hydrological response to rainfall. For instance, urbanization often results in increased impervious surfaces and reduced infiltration, leading to higher and faster runoff. The topography of an area also plays a role; steep slopes can cause rapid runoff and erosion, while flat land may allow water to puddle and evaporate before it contributes to runoff. Furthermore, antecedent moisture conditions are significant, as the soil's moisture content before a rainfall event influences runoff behavior. Saturated soil reduces infiltration and leads to increased runoff. Lastly, measuring rainfall runoff through satellite data introduces its own challenges, as remote sensing techniques come with limitations and uncertainties that must be considered.

Measuring rainfall-runoff using satellite data presents several challenges. First, the spatial and temporal resolution of satellite data may be insufficient to capture the detailed hydrological processes that influence runoff, often being too coarse to detect small-scale variations in rainfall and runoff. Additionally, satellite measurements typically cover only limited areas, which may not represent the entire catchment, complicating efforts to extrapolate results, particularly in regions with complex topography. Calibration and validation

of satellite data against ground-based measurements are essential for ensuring accuracy, but this process can be challenging due to the limited number of ground observations. Furthermore, cloud cover and atmospheric interference can significantly impact the accuracy of satellite-based rainfall measurements, as clouds may obscure the satellite's view of the Earth's surface, while atmospheric elements, such as water vapor, can distort readings. The cost and limited availability of satellite data, especially in developing countries, can hinder widespread use. Finally, the algorithms employed to derive rainfall-runoff from satellite data have inherent limitations and uncertainties; different algorithms may yield varying results, and their accuracy can be influenced by the location and type of rainfall event. While satellite-based measurements of rainfall-runoff have the potential to provide valuable insights, they come with their own set of challenges that need to be addressed to ensure their accuracy and reliability. Proper calibration, validation, and careful interpretation of the results are necessary to obtain meaningful insights from satellite-based measurements.

Our research work considered the following challenges and problems:

- Spatial and temporal resolution, data availability, land use, and limited coverage are needed to provide the solution.
- Most of the research work considered a small regional area for their study in rainfall-runoff estimation.
- No comparison is provided based on the metrology department's data in most of the research work.
- Finding the variation in the precipitation and runoff for every year and month will assist the researchers in performing predictions.

Based on the challenges, discussed above, a system is proposed to estimate the rainfall-runoff and precipitation for Andhra Pradesh from 2015 to 2021 by applying the SCS curve number technique to the land and land cover data and the soil texture class. The variation in precipitation and runoff for every year and the correlation among the years in rainfall is analyzed and presented. The remainder of the paper is organized as follows: Section 2 provides a comprehensive analysis of the various methods developed for estimating and assessing rainfall, runoff, and precipitation in a specific region. Section 3 covers the data collection, study area and methodologies used in this research. Section 4 explains the system model, architecture, and working principles of the current study. Section 5 describes the results produced by the proposed model and offers a detailed comparative analysis. Finally, Section 6 concludes the paper and discusses future directions.

## 2. Literature Review

Zhang et al. (2011) proposed a NRCS-CN approach for calculating watershed runoff and risk of disasters, which produced 90.8% accuracy. When runoff is poor, this strategy is useless for reducing errors. Ahmad et al. (2022) analyzed the long-term variation in rainfall and trends using satellite data by employing artificial neural networks. In Gujrat, the

maximum annual rainfall was found with a statistically significant upward trend (50.8 mm/decade). Wetchayont et al. (2023) used the geostatistical method to estimate rainfall in Bangkok by utilizing satellite, radar, and gauge rainfall datasets. In this work, the mean estimated rainfall ranged from 0.0012 to 3.80 mm h<sup>-1</sup> and 0.02 to 2.53 mm h<sup>-1</sup>. Gupta et al. (2022) used the NRCS-CN approach while integrating GIS and remote sensing. The normal runoff depth and mean annual precipitation ranges are 444.50 to 1960 mm and 936 to 3520 mm, respectively. Fowler et al. (2022) described how rainfall-runoff interactions changed before, during, and after Australia's Millennium Drought. The Millennium Drought and droughts from 1950 to 1990 are contrasted with two droughts that occurred before 1950. Saragih et al. (2022) used observational rainfall data from Central MKG Region I Medan to evaluate the CHIRPS rainfall estimation data. November 2018 saw the highest CHIRPS monthly correlations of 0.520. Raza et al. (2023) proposed Irrigation Management Using GIS, which could help to comprehend rainfall calculation is that it measures the transference of soil, plants, and environment and produced accuracy 75.47%. Hassan et al. (2022) proposed a Machine Learning algorithm for Radar-Based Rainfall Assessment. The investigation also revealed that the RMG and RBRT(RC) estimators significantly overestimate the overall seasonal rainfall accumulation by around 60%. Soulis and Valiantzas (2012) proposed a rainfall estimation model, which will reduce the relative error to 3.18% and accounts for 43.5% of the precipitation estimate without filter wave calibration. Liu et al. (2023) suggested a deep learning-based approach to assess the impact of artificial precipitation, produced residual rainfall 9.98 mm in Shiyan region on 26th April 2018. Seong et al. (2022) Proposed Grid Rainfall-Runoff Model (GRM) for assessment of Uncertainty measures, which produced logarithmic Nash-Sutcliffe Efficiency 0.97. Loveridge and Rahman (2021) proposed Monte Carlo method to find variability in design flood estimates; it reduces the relative error to 3%. Sishah (2021) used SCS-CN approach to assess the rainfall runoff in the awash river basin located in Ethiopia, the correlation coefficient of 0.9253 is produced between the anticipated runoff and the actual runoff. Moglen et al. (2022) used the NRCS Curve Number Technique for Determining the Curve Number from Rainfall-Runoff values; it produced the mixed value from 0.05 to 0.20. Gholami and Khaleghi (2021) modelled the rainfall-runoff mechanism using a multilayer perceptron (MLP) network. For the date 15th, 1995, the correlation between the observed and simulated values is 0.6, and the correlation between the observed and simulated information is 0.6. Mohammadi et al. (2022) proposed a multi-conceptual method using machine learning for runoff and rainfall predictions, the model produced the accuracy of 68% of NSE.

### 3. Materials and Methods

#### 3.1 Dataset

The Terra and Aqua combined Moderate Resolution Imaging Spectroradiometer (MODIS) Land Cover Type (MCD12Q1) Version 6.1 data package provides global land cover categories at yearly intervals from 2001 to 2021

(<https://lpdaac.usgs.gov/products/mcd12q1v061/#tools>). The MCD12Q1 V 6.1 data product is generated using trained classifications of MODIS. For information on soil texture categories (USDA system) for six typical soil depths, another dataset, called OpenLand Map Soil Texture Class (USDA System)([https://developers.google.com/earth-engine/datasets/catalog/OpenLandMap\\_SOL\\_SOL\\_TEXTURE-CLASS\\_USDA-TT\\_M\\_v02](https://developers.google.com/earth-engine/datasets/catalog/OpenLandMap_SOL_SOL_TEXTURE-CLASS_USDA-TT_M_v02)), is used to derive from the soil texture package in R's expected soil texture fractions. One of the Curve Number approaches is mainly used in the current case research, which assumes determining the catchment's surface runoff. Calculating the amount of runoff from the land surface that enters rivers or streams is made more accessible by using the SCS-CN approach. The dataset, used as the rainfall dataset, is "CHIRPS Daily: Climate Hazards Group InfraRed Precipitation with Station data (Version2.0Final)" ([https://developers.google.com/earth-engine/datasets/catalog/UCSB-CHG\\_CHIRPS\\_DAILY](https://developers.google.com/earth-engine/datasets/catalog/UCSB-CHG_CHIRPS_DAILY)). A 30+ year quasi-global rainfall dataset is available under Climate Hazards Group InfraRed Precipitation with Station Data (CHIRPS), combining in-situ station data with 0.05° resolution satellite imagery.

#### 3.2 Study Area

The present study concerns the state of Andhra Pradesh in India. As shown in Figure 1, the state is located in India's south-eastern coastline region. Its 162,975 km<sup>2</sup> make it the seventh-largest state in terms of size (62,925 sq mi).

The terrain of the state is diverse, spanning from the Nallamala Hills and Eastern Ghats Hills to the Bay of Bengal coastlines, which sustain a wide range of ecosystems and a vast diversity of flora and animals. The state is traversed by its two principal rivers: the Krishna and Godavari. The state's 975-km-long coastline stretches across the Bay of Bengal from Srikakulam to Nellore (606 mi). The entire population is made up of 14,610,410 urban residents and 34,776,389 rural residents, for a population share of 29.6%. Andhra Pradesh's economy is mostly dependent on agriculture and cattle. Four large Indian rivers—the Godavari, Krishna, Penna, and Tungabhadra—provide irrigation and pass through the state. 60 percent of the population works in agribusiness and associated sectors. Rice is the state's primary food crop and staple diet.

#### 3.3 Data Pre-processing

In this study, using statistics and data processing on the MODIS/061/MCD12Q1 dataset, gridded rainfall products that are available weekly, seasonally, and annually were extracted, deploying the GEE platform using the 'ee.ImageCollection' technique and the filter command (ee.Filter.calendarRange). The 'clip' function was then applied to restrict the field of study and obtain relevant information in accordance with the field of study. The dataset SOL\_TEXTURE-CLASS\_USDA-TT\_M/v02 is processed to determine soil classes and convert hydrological soil categories like A, B, C, and D depending on their infiltration capacity. The operation 'ee.Filter.date' is applied to the CHIRPS dataset to filter the daily rainfall information for the specified duration.

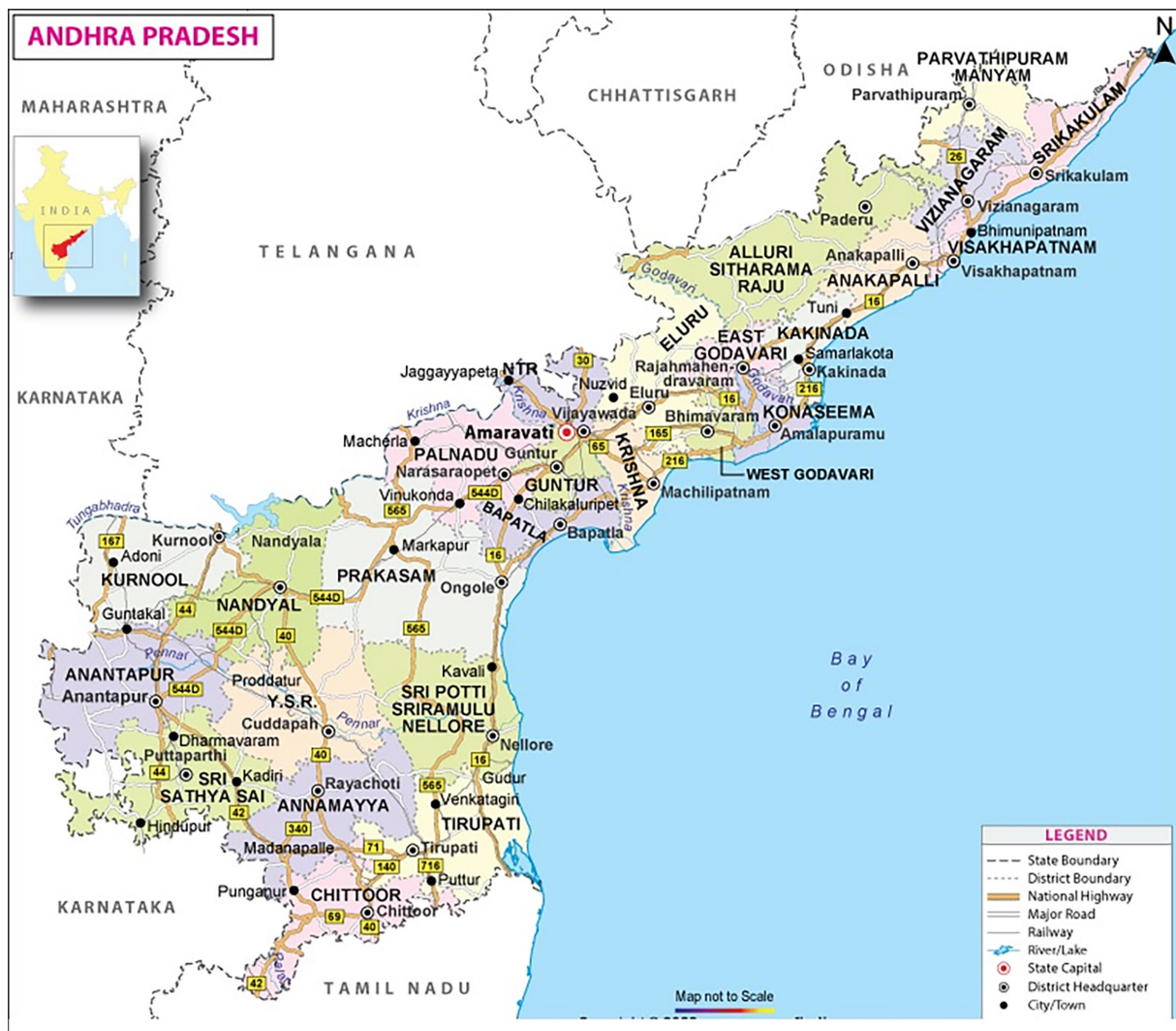


Figure 1. Map of the state of Andhra Pradesh

### 3.4 Methods

#### 3.4.1 Curve Number (CN) Method

A common hydrological approach for calculating direct runoff from rainfall events in watershed modelling is the Curve Number (CN) method. It was created as a component of the Soil Conservation Service (SCS) methodology. The quantity of rainfall that results in direct runoff is estimated using the CN technique, which takes into account a number of variables including soil type, land use, and prior soil moisture conditions. It is particularly useful in predicting surface runoff in agricultural and urban areas. The CN method involves the following steps:

1. Determine Soil Hydrological Group: Soils are categorized into four hydrological classes (A, B, C, and D) depending on their infiltration features. These groups are assigned according to soil properties like texture, permeability, and depth. Each group has a corresponding range of CN values.
2. Assign Land Use Category: Different land use or land cover types within the watershed are classified into specific categories. Examples of land use categories include forest, agriculture, urban, and grassland. Each land use category has an associated CN value range.

3. Establish Antecedent Soil Moisture Condition: Antecedent soil moisture is the amount of moisture in the soil prior to a rainfall occurrence, which affects the runoff response. Antecedent soil moisture conditions are classified into three categories: dry, normal, and wet. Each condition has a corresponding adjustment factor applied to the CN value.
4. Determine Curve Number (CN): Once the hydrological group, land use category, and antecedent soil moisture condition are known, the CN value is determined. This is typically done using lookup tables the SCS provides or through equations specific to the region or application.
5. Calculate Direct Runoff: With the CN value determined, the rainfall data for a specific event can be utilized to calculate the direct runoff.

### 4. Research Methodology

#### 4.1 System Model

Two key theories have been put forth, and the SCS-CN technique depends on the water balance computation. The SCS-CN method is not represented by a single mathematical model but rather a set of equations and lookup tables. The process is based on empirical relationships and lookup tables

developed by SCS. These relationships are used to calculate direct runoff from precipitation occurrences depending on the hydrological, soil, and use of land factors. As shown in equation (5), the Curve Number (CN) parameter must be determined based on soil and land use characteristics. The CN value is typically determined using lookup tables provided by the SCS or through equations that consider the soil hydrological features and land use factors. The CN value is influenced by three key factors: Land usage, soil type, and previous soil moisture levels. This method assigns different CN values to different combinations of these factors, ranging from 0 to 100. Lower CN scores represent greater significance infiltration rates, while greater CN values indicate lower infiltration rates. The SCS-CN method provides lookup tables or equations to determine the CN value based on the soil hydrological group (A, B, C, or D), land use category (such as forest, agriculture, urban), and antecedent soil moisture condition (dry, normal, or wet). These lookup tables or equations vary depending on the region and specific application.

#### 4.2 Architecture and working

The SCS-CN method does not have a specific architecture. Instead, it is a conceptual framework or methodology for calculating direct runoff from rainfall occurrences based on soil, land use, and hydrological features. The SCS-CN method involves the following key components:

- **Rainfall Data:** Rainfall data, such as precipitation depth and intensity, is collected or obtained for the field of study. This data serves as input to the SCS-CN method.
- **Soil Hydrological Group:** The SCS-CN method classifies soils into hydrological categories (A, B, C, or D) depending on their infiltration properties. The hydrological group is determined based on soil texture, permeability, and other soil characteristics. Lookup tables or equations are used to assign the appropriate hydrological group to each soil type in the field of study.
- **Land Use Categories:** Land use or land cover information is considered in the SCS-CN method as it affects the amount of runoff generated. Different land use categories, such as forest, agriculture, or urban areas, have different runoff characteristics. Lookup tables or equations are used to assign the appropriate land use category to each area within the study area.
- **Antecedent Soil Moisture Conditions:** The SCS-CN method considers the antecedent soil moisture conditions, which represent the moisture content in the soil before a rainfall occurrence. These conditions can be classified as dry, normal, or wet. Lookup tables or equations assign the appropriate antecedent soil moisture condition to each area within the study area.
- **Curve Number (CN):** It represents the cumulative impact of soil type, use of the property, and previous soil wetness conditions on the runoff process.
- **Direct Runoff Calculation:** The SCS-CN method uses the CN value and rainfall data to calculate the direct runoff from rainfall occurrences.

To estimate the direct runoff in the study region, empirical methods like the SCS-CN methodology are typically utilized as shown in Figure 2. Another cloud-based computing platform is GEE, which integrates Google's computational infrastructure with freely available GIS and remote sensing datasets. Any user can use any web browser to access GEE. It is freely accessible to everyone and effectively handles massive data thanks to automatic parallel processing. The vast collection of spatial data that GEE offers makes it easier to choose input data. Users can select their datasets from big sets of image collections using various filter techniques.

The SCS—CN equation is written by

$$Q = (P - I_a)^2 / P - I_a + S \quad \text{for } P > I_a \quad (1)$$

$$Q = 0 \quad \text{for } P < I_a \quad (2)$$

where  $P$  represents daily rainfall,  $I_a$  original simplification,  $F$  represents effective retention,  $Q$  represents straight surface run-off, and  $S$  represents the possible maximum durability. CN1, CN2, and CN3 values are calculated using the formula. Soil texture is converted into 4 types of soil groups: A == 1, B == 2, C == 3, and D == 4, where  $S$  is measured in millimeters and CN is a dimensionless run-off coefficient that is influenced by the type of soil, the use of the land, and the preexisting moisture conditions (AMC). The relative levels of dryness or moisture of a watershed, which varies continuously and has a big impact on run-off, is known as antecedent moisture.

Depending on the LULC and the soil category characteristics, CNs has been proposed. CN can be derived from the following equations:

$$CN1 = CN2 / (2.281 - (0.0128 * CN2)) \quad (3)$$

$$CN3 = CN2 / (0.427 + (0.00573 * CN2)) \quad (4)$$

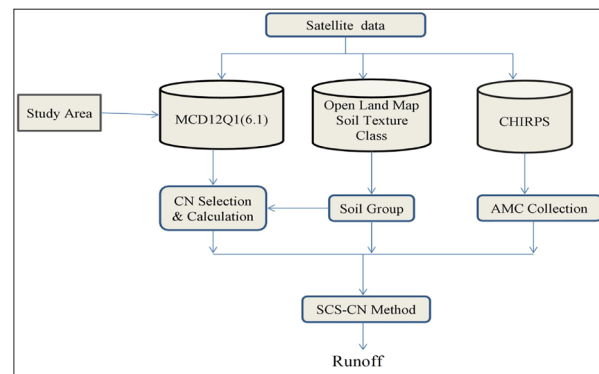


**Figure 2.** Overall flow diagram to estimate the rainfall-runoff

The required datasets, MCD12Q1 version 6.1 for land cover types, OpenLandMap Soil Texture Class for classifying the soil texture groups, and Climate Hazards Group Infrared Precipitation with Station Data (Version 2.0), are imported to the GEE through the JavaScript API. The soil texture map is transformed into different kinds of soil categories.

#### Procedure:

1. The required datasets are imported into GEE through the JavaScript API.
2. The soil texture map is transformed into different kinds of hydrologic soil groups, A, B, C, and D.
3. Curve number selection is done for all possible parameters of the four soil types and the LULC data

categories.

4. Daily rainfall information pictures are used to make daily AMC pictures.
5. To estimate run-off (Q), the equation (1) is used.

## 5. Results and Analysis

### 5.1 Experimental Setup

The experiment in this study is carried out using the Google Earth Engine platform. The GEE comprises a high-performance, intrinsically catalog computing service, and

a multi-petabyte data catalog that is ready for examination. It may be accessed and managed online thanks to an application programming interface (API) and a web-based interactive development environment (IDE) that facilitate quick prototyping and result visualization as shown in Figure 3. The public data catalogue for the Earth Engine is a multi-petabyte curated collection of extensively used geospatial datasets. Earth-observing remote sensing images make up the majority of the catalog.

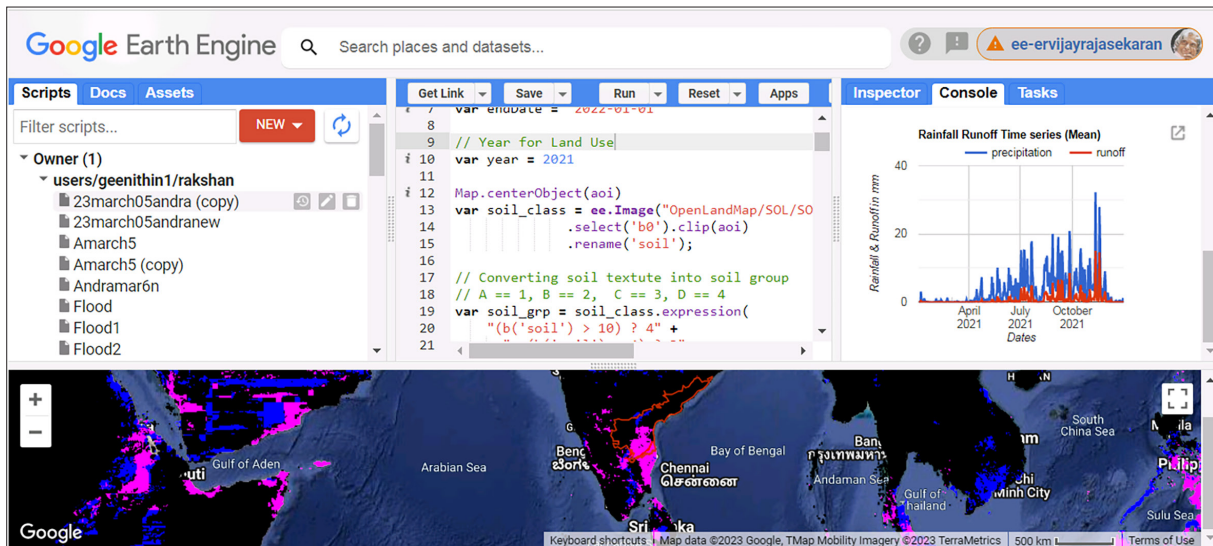


Figure 3. Experiment setup on the GEE platform

### 5.2 Performance Metrics

The rainfall runoff based on soil type, land use, antecedent moisture conditions, and rainfall characteristics is calculated using precipitation and retention values. The formula for calculating the rainfall runoff is given in Equation 5:

$$\text{Runoff} = \frac{(\text{Precipitation} - \text{The potential maximum retention} * 0.2)^2}{(\text{Precipitation} + \text{The potential maximum retention} * 0.8)} \quad (5)$$

The percent error formula for calculating the accuracy of precipitation is shown in equation 6:

$$\text{Percent Error} = \frac{(\text{Observed Value} - \text{Predicted/Measured Value})}{(\text{Predicted/Measured Value})} * 100 \quad (6)$$

The “Observed Value” refers to the actual or observed precipitation amount. “Predicted / Measured Value” refers to the predicted or measured precipitation amount. The numerator of the formula calculates the difference between the observed and predicted/measured values. The denominator represents the predicted/measured value. The result is multiplied by 100 to obtain the percentage value. By calculating the percent error, you can determine the accuracy of the precipitation prediction or measurement. A lower percent error indicates a higher level of accuracy, while a higher percent error indicates a more significant deviation between the observed and predicted / measured values.

### 5.3 Results

#### 5.3.1 Yearly Rainfall Analysis

Both the rainfall and runoff have followed a similar pattern: they began to rise in the middle of August, peaked in November, and then began to decline by the end of December. The total runoff for the year 2021 is 172.459. The maximum runoff value is 26.523, and the precipitation value is 47.222,

which was observed on November 11, 2021. And second, the maximum runoff value is 24.102; the precipitation value is 43.711, which was observed on November 18<sup>th</sup>, 2021 as shown in Figure 4.

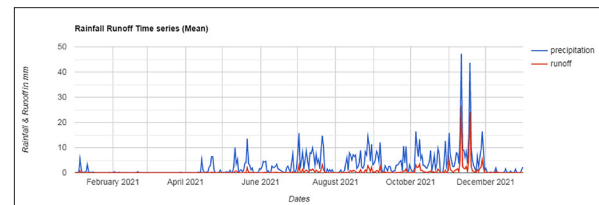


Figure 4. Time Series Plots of Yearly Rainfall Data for Andhra Pradesh State for the Year 2021

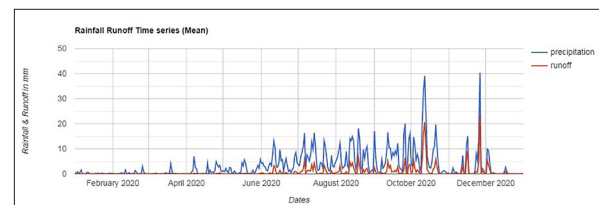
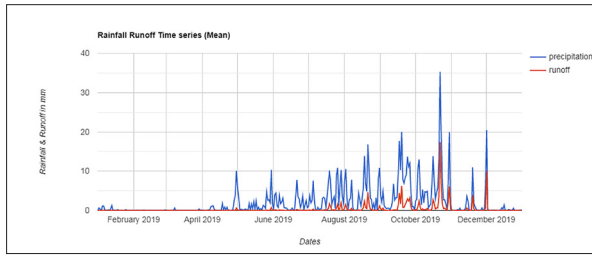


Figure 5. Time Series Plots of Yearly Rainfall Data for Andhra Pradesh State for the Year 2020

Similar trends in rainfall and runoff have been observed; both began increasing in August. The maximum runoff value is 20.677, and the maximum precipitation value is 39.107, observed on October 12<sup>th</sup>, 2020, as shown in Figure 2. The maximum precipitation value of 39.107 was also observed on October 12<sup>th</sup>, 2020, as shown in Figure 5.



**Figure 6.** Time Series Plots of Yearly Rainfall Data for Andhra Pradesh State for the Year 2019

The total runoff and precipitation values for the year 2019 are 127.438 and 812.097. The maximum runoff value is 17.377 and the maximum precipitation value is 35.268, which were observed on October 22, 2019. And second, the maximum runoff value is 9.98 and the maximum precipitation value is 20.466, which were observed on December 1, 2019 as shown in figure 6.

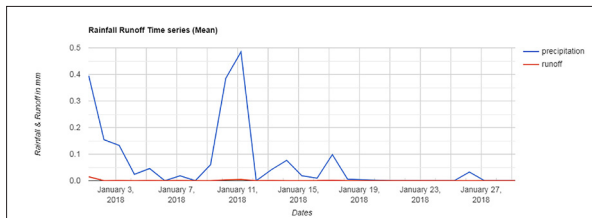


**Figure 7.** Time Series Plots of Yearly Rainfall Data for Andhra Pradesh State for the Year 2018

The total runoff and precipitation values for the year 2018 were 183.763 and 1198.909. The average runoff and precipitation values for the year 2018 were 0.50623 and 3.30278. The highest precipitation and runoff values of 12.914 and 30.604 occurred on November 16, 2018, with the dates of November 10, January 5, 6, and 7 receiving 0 runoff and precipitation as shown in Figure 7.

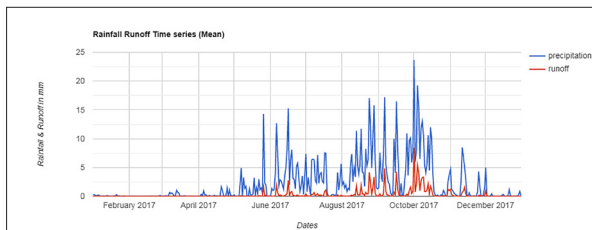


**Figure 8.** Time Series Plots of Yearly Rainfall Data for Andhra Pradesh State for the Year 2017

The total runoff and precipitation values for the year 2017 are 105.559 and 830.005. The average runoff and the amount of precipitation that fell in the year 2017 are 0.289203 and 2.273986. The highest precipitation and runoff values of 23.681 and 8.402 occurred on October, 2017, with the dates of November 8, 9 and 18 receiving 0 runoff and precipitation as shown in Figure 8. The total runoff and precipitation values for the year 2016 are 63.49 and 591.33. The average runoff and precipitation values for the year 2016 are 0.17 and 1.615. The highest precipitation and runoff values of 19.225 and 8.046 occurred on December 12, 2016, with the dates of November 5, January 14, 18, and 28 receiving 0 runoff and precipitation as shown in Figure 9. The total runoff and precipitation values for the year 2015 are 124.612 and 783.482. The highest precipitation and runoff values

of 38.225 and 18.20 occurred on December 18, 2015, with the dates of November 5, January 10, 14, and 18 receiving 0 runoff and precipitation as shown in Figure 10.

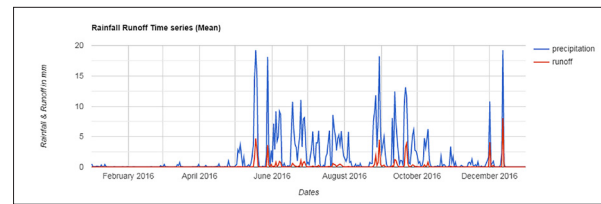


**Figure 9.** Time Series Plots of Yearly Rainfall Data for Andhra Pradesh State for the Year 2016

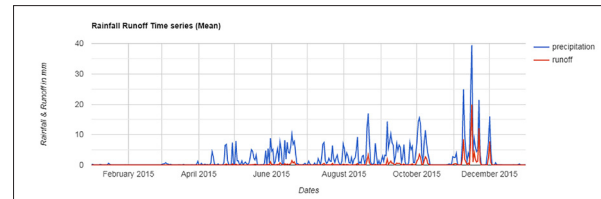


**Figure 10.** Time Series Plots of Yearly Rainfall Data for Andhra Pradesh State for the Year 2015

**5.3.2 Monthly Rainfall Analysis**

October and November months are taken into consideration for an in-depth analysis of rainfall. The total runoff and the amount of precipitation that fell in November 2021 are 99.05 and 283.372. The average runoff and the amount of precipitation that fell in November 2021 are 9.44 and 3.301. The total and average runoff values for the month of September are 9.08 and 0.30. The total runoff and the amount of precipitation that fell in November 2020 are 50.614 and 115.087. The average runoff and the amount of precipitation that fell in November 2020 are 1.687 and 3.836. The highest precipitation and runoff values of 40.333 and 23.346 occurred on November 26, 2020, with the dates of November 18, 19, and 20, receiving 0 runoff and precipitation as shown in Figures 11 and 12.

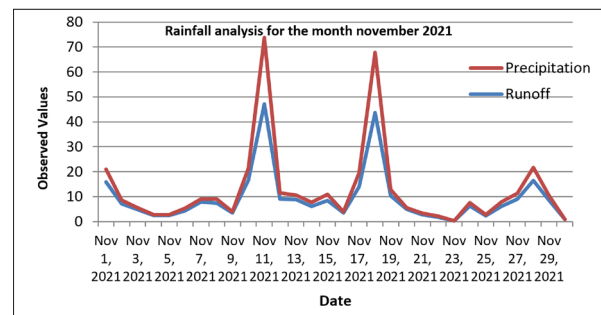


**Figure 11.** Rainfall analysis for the month of November 2020

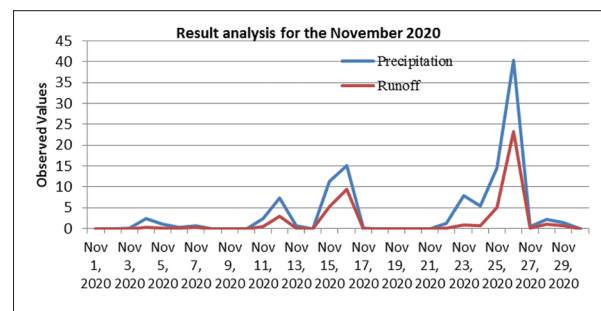


**Figure 12.** Rainfall analysis for the month of November 2020–2021



The total runoff and the amount of precipitation that fell in November 2019 are 6.16 and 29.539. The average runoff and the amount of precipitation that fell in November 2019 are 0.2 and 0.98, respectively. The total and average runoff values for the month of October are 51.163 and 1.65, respectively. The total and average runoff values for the month of September are 30.127 and 1.004 as shown in Figure 13.

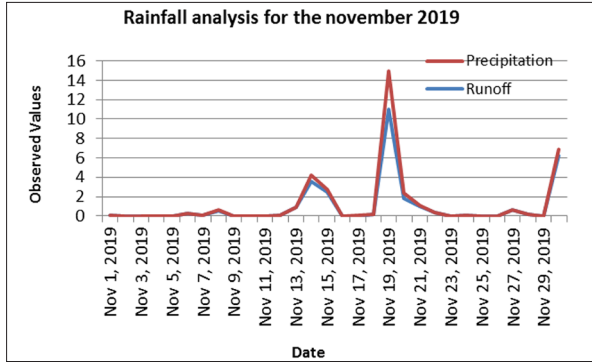


Figure 13. Rainfall analysis for the month of November 2019

The total runoff and the amount of precipitation that fell in November 2018 are 45.681 and 155.04539. The average runoff and the amount of precipitation that fell in November 2018 are 5.168 and 1.5227. The highest precipitation and runoff values of 30.604 and 12.914 occurred on November 16, 2018, with the dates of November 10, 25, and 27 receiving 0 runoff and precipitation as shown in Figure 14.

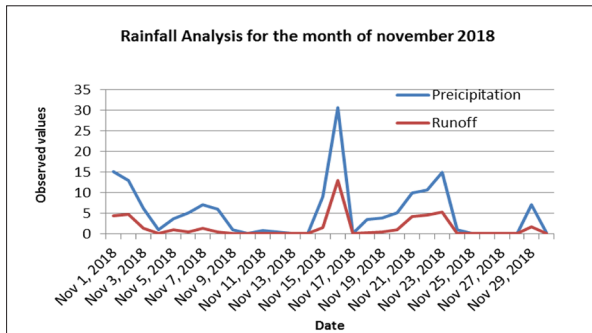


Figure 14. Rainfall analysis for the month of November 2018

The total runoff and the amount of precipitation that fell in November 2017 are 5.893 and 43.598. The average runoff and the amount of precipitation that fell in November 2017 are 0.1964 and 1.53, respectively. The highest precipitation and runoff values of 4.699 and 1.198 occurred on November 1, 2017, with the dates of November 8, 9, and 18 receiving 0 runoff and precipitation as shown in Figure 15.

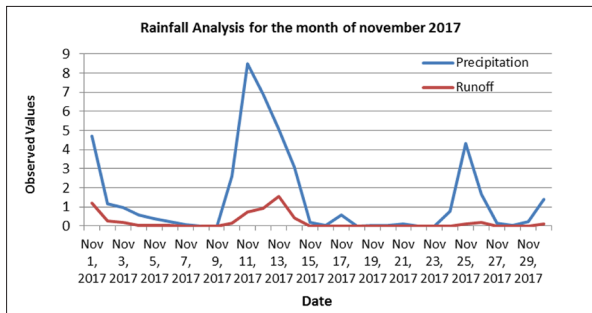


Figure 15. Rainfall analysis for the month of November 2017

The total runoff and the amount of precipitation that fell in November 2016 are 63.49 and 591.333. The average runoff and the amount of precipitation that fell in November 2016 are 0.17347 and 1.615664. The highest precipitation and runoff values of 19.225 and 8.046 occurred on December 12, 2016, with the dates of November 30 and 31 receiving 0 runoff and precipitation as shown in Figure 16.

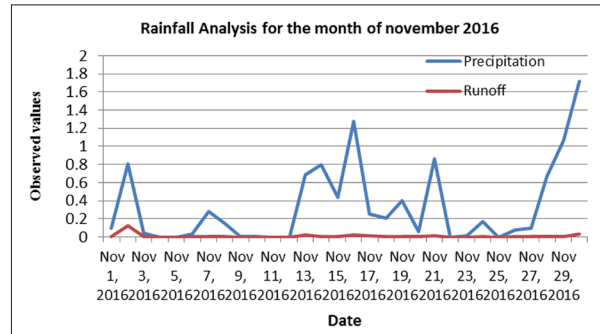


Figure 16. Rainfall analysis for the month of November 2016

The total runoff and the amount of precipitation that fell in November 2015 are 68.518 and 193.327. The average runoff and the amount of precipitation that fell in November 2015 are 0.544 and 2.99, respectively. The highest precipitation and runoff values of 39.466 and 19.905 occurred on November 16, 2015, with the dates of November 5 and 27 receiving 0 runoff and precipitation, as shown in Figure 17.

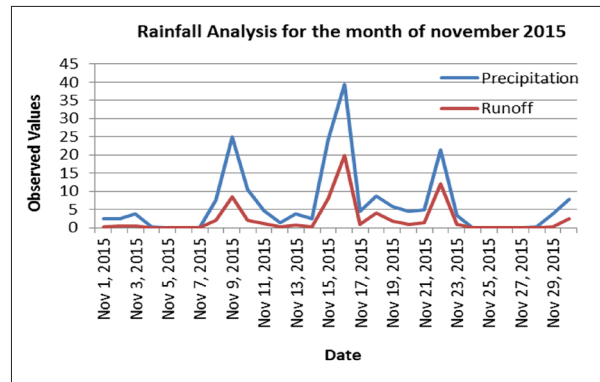
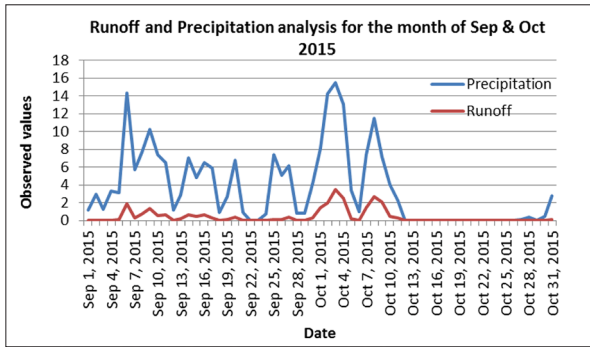


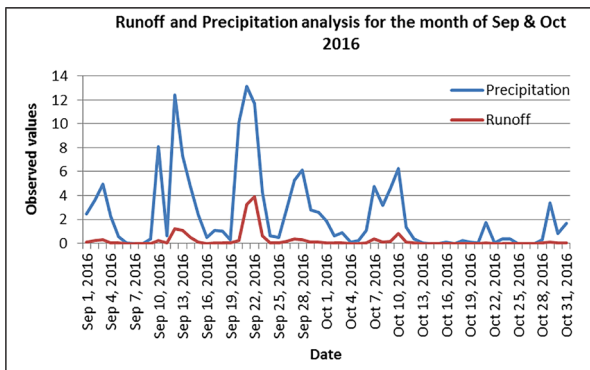
Figure 17. Rainfall analysis for the month of November 2015

Figure 18 shows the total runoff and the amount of precipitation that fell in September 2015 are 9.577 and 128.524. The average runoff and the amount of precipitation that fell in September 2015 are 0.319 and 4.28, respectively. The highest precipitation and runoff values of 14.356 and 1.934 occurred on September 6, 2015, with the dates of September 23 receiving 0 runoff and precipitation. The total runoff and the amount of precipitation that fell in October 2015 are 16.859 and 91.418. The average runoff and the amount of precipitation that fell in October 2015 are 0.544 and 2.99, respectively. On October 3, 2015, the highest precipitation and runoff values were 15.464 and 3.479 respectively, with October 13, 18, 21 to 25 receiving 0 precipitation runoff values.



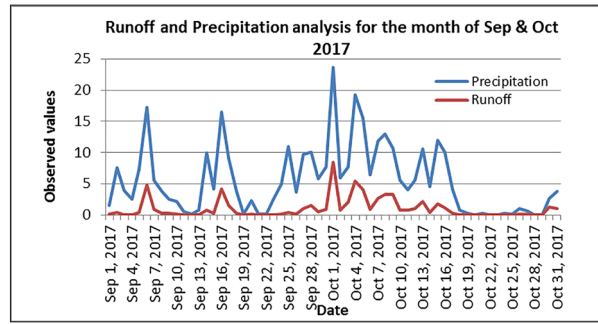
**Figure 18.** Runoff and precipitation analysis for Sep & Oct 2015

Figure 19 shows the total runoff and the amount of precipitation that fell in September 2016 are 13.068 and 112.718. The average runoff and the amount of precipitation that fell in September 2016 are 0.44 and 3.76. The highest precipitation and runoff values of 13.135 and 3.889 occurred on September 21 2016, with the dates of September 7 and 8 receiving 0 runoff and precipitation. The total runoff and the amount of precipitation that fell in October 2016 are 1.991 and 34.555. The average runoff and the amount of precipitation that fell in October 2016 are 0.064 and 1.114. The highest precipitation and runoff values of 6.236 and 0.807 occurred on October 10 2016, with the dates of October 14, 15, 17, and 25 to 27.



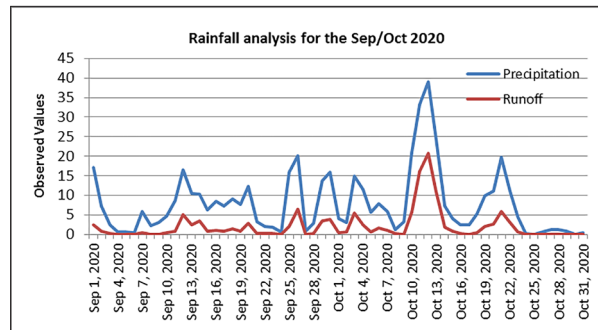
**Figure 19.** Runoff and precipitation analysis for the month of Sep & Oct 2016

Figure 20 shows the total runoff and the amount of precipitation that fell in September 2017 are 18.951 and 156.636. The average runoff and the amount of precipitation that fell in September 2017 are 5.22 and 0.6317. The highest precipitation and runoff values of 17.2 and 4.849 occurred on September 6 2017, with the dates of September 19 receiving 0.0001 and 0.094 runoff and precipitation. The total runoff and the amount of precipitation that fell in October 2017 are 41.794 and 180.108. The average runoff and the amount of precipitation that fell in October 2017 are 1.384 and 5.81, respectively. The highest precipitation and runoff values of 19.242 and 5.417 occurred on October 4 2017, with the dates of October 23 receiving 0 runoff and precipitation.



**Figure 20.** Runoff and precipitation analysis for the month of Sep & Oct 2017

Figure 21 shows the total runoff and the amount of precipitation that fell in September 2018 are 42.228 and 223.995. The average runoff and precipitation that fell in September 2018 are 3.766 and 0.438, respectively. The highest precipitation and runoff values of 2.336 and 11.972 occurred on September 16, 2018, with the dates of September 7 receiving 0 runoff and precipitation. The total runoff and the amount of precipitation that fell in October 2018 are 57.604 and 211.428. The average runoff and precipitation that fell in October 2018 are 1.203 and 6.254, respectively. On October 5, 2018, the highest precipitation and runoff values were 24.812 and 9.738 respectively, with October 30 receiving 0.293 precipitation and 0.011 runoff values.



**Figure 21.** Runoff and precipitation analysis for the month of Sep & Oct 2018

The total runoff and the amount of precipitation that fell in September 2018 are 33.772 and 208.728. The average runoff and the amount of precipitation that fell in September 2018 are 1.004233 and 5.522867, respectively. The highest precipitation and runoff values of 19.957 and 6.219 occurred on September 19, 2019, with the dates of September 30 receiving 0.018 runoff and 0.095 precipitations. The total runoff and the amount of precipitation that fell in October 2019 are 68.571 and 254.534. The average runoff and the amount of precipitation that fell in October 2019 are 1.650419 and 6.824129, respectively. On October 22, 2019, the highest precipitation and runoff values were 35.268 and 17.377, respectively, with October 28 receiving 0.268 precipitation and 0.017 runoff values, as shown in Figure 22.

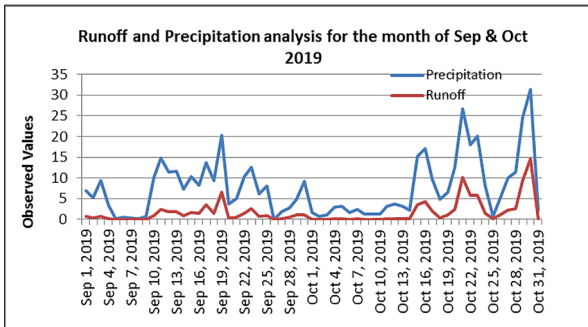


Figure 22. Runoff and precipitation analysis for the month of Sep & Oct 2019

The total runoff and the amount of precipitation that fell in September 2020 are 40.759 and 217.792. The average runoff and the amount of precipitation that fell in September 2020 are 1.3586 and 7.2597, respectively. The highest precipitation and runoff values of 20.136 and 6.492 occurred on September 26, 2020, with the dates of September 6 receiving 0.001 and 0.0338 runoff and precipitation respectively. The total runoff and the amount of precipitation that fell in October 2020 are 82.939 and 256.494. The average runoff and the amount of precipitation that fell in October 2020 are 2.675 and 8.274, respectively. On October 12, 2020, the highest precipitation and runoff values were 30.109 and 20.677 respectively, with October 25 receiving 0 precipitation and 0 runoff values as shown in Figure 23.

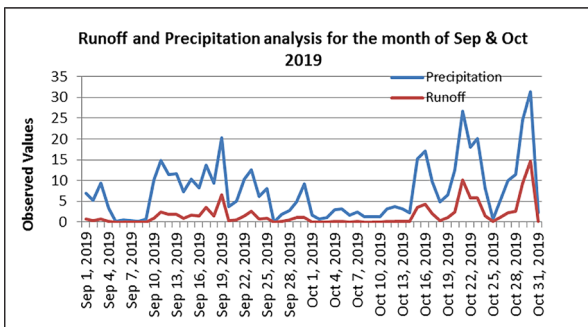


Figure 23. Runoff and precipitation analysis for Sep & Oct 2020

The total runoff and the amount of precipitation that fell in September 2021 are 9.088 and 105.518. The average runoff and the amount of precipitation that fell in September 2021 are 0.303 and 3.517, respectively. The highest precipitation and runoff values of 12.104 and 2.574 occurred on September 6, 2021, with the dates of September 16 receiving 0 and 0.195 runoff and precipitation, respectively. The total runoff and the amount of precipitation that fell in October 2021 are 20.475 and 145.872. The average runoff and the amount of precipitation that fell in October 2021 are 0.66 and 4.706, respectively. On October 5, 2021, the highest precipitation and runoff values were 16.397 and 3.424 respectively, with October 25 and 26 receiving 0.001 precipitations and 0 runoff values as shown in Figure 24.

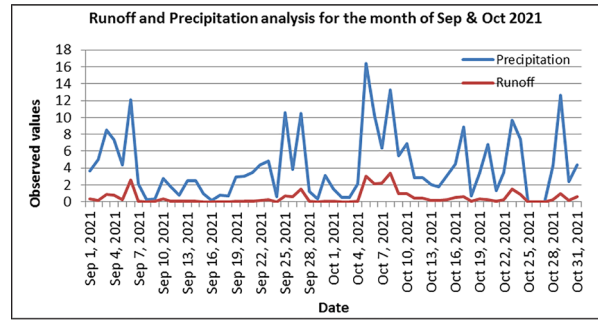


Figure 24. Runoff and precipitation analysis for the month of Oct & Nov 2021

5.4 Analysis

Table 1 shows the total runoff results computed for the years 2015–2021, which are 172.459; 209.666; 105.599; 63.49; and 124.612, respectively. The year 2020 has the highest runoff (209.666 percent), and the year 2016 has the lowest runoff (63.49 percent). As shown in Figure 25, the year 2018 has the highest precipitation of 1198.909 and the lowest precipitation of 591.33, and other precipitation values are 993.976, 1104.7, 812.097, 830.005, and so on. Table 2 shows the runoff and precipitation for the three months of September through November from 2015 to 2021. The month of September of the year 2020 received the highest precipitation value of 217.792. It shows that there will be a good correlation like 100 among the precipitation (105.518 to 156.636) and runoff (9.088 to 33.772) for the years 2015 to 2021, except for 2020. The years 2016 and 2018 have very near precipitation values of 112.718 and 112.968 in the month of September.

Table 1. Year-Wise Analysis (2015–2021)

Year	Runoff	Precipitation
2021	172.459	993.976
2020	280.889	1276.32
2019	127.438	812.097
2018	183.763	1198.909
2017	105.599	830.005
2016	63.49	591.33
2015	124.612	783.482

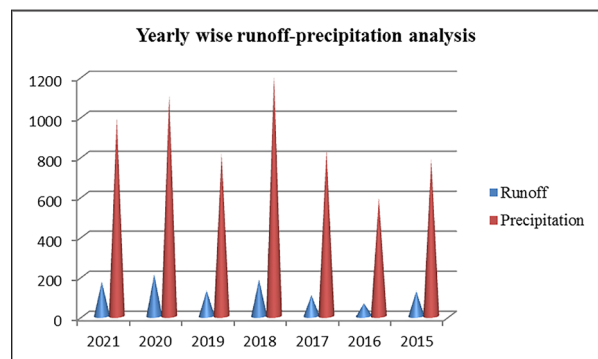
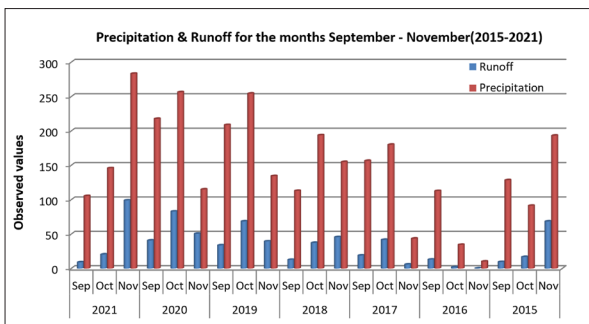


Figure 25. Year-wise runoff-precipitation analysis

**Table 2.** Three-month analysis for the years 2015-2021

Year	Month	Runoff	Precipitation
2021	Sep	9.088	105.518
	Oct	20.475	145.872
	Nov	99.05	283.372
2020	Sep	40.759	217.792
	Oct	82.939	256.494
	Nov	50.614	115.087
2019	Sep	33.772	208.728
	Oct	68.571	254.534
	Nov	39.466	134.546
2018	Sep	12.669	112.968
	Oct	37.3	193.88
	Nov	45.681	155.045
2017	Sep	18.951	156.636
	Oct	41.794	180.108
	Nov	5.893	43.598
2016	Sep	13.068	112.718
	Oct	1.991	34.555
	Nov	0.283	10.225
2015	Sep	9.577	128.524
	Oct	16.859	91.418
	Nov	68.518	193.327

As shown in Figure 26, November 2016 received a very low rainfall precipitation 10.225 than all the years. November 2021 received 283.372 highest precipitations. November has more variations in terms of runoff and precipitation values. There is a good correlation among the years 2016, 2018, and 2021 in September. The month of October 2016 received a very low precipitation value of 34.555 compared to all the years, and the year 2020 received the highest value for its October month of 256.494. There is more variation for the month of October in terms of its precipitation and runoff values.



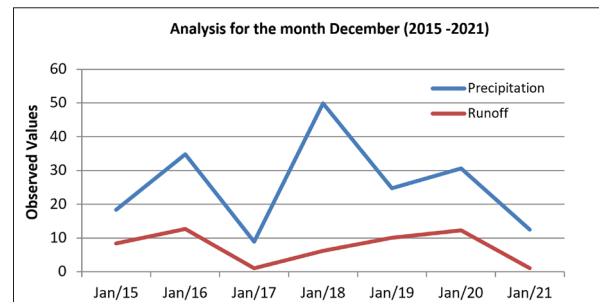
**Figure 26.** Three-month analysis for the months September – November

Figure 26: As shown in Table 3, there are abrupt changes in the precipitation values for the years 2016, 2017, 2018, and 2021. December of 2015 has received 18.352 mm; year 2016 has received more precipitation, 34.78 mm, which is 16.428 mm higher than 2015. December 2017 received a very low precipitation value of 8.932, which is less precipitation than the previous years. December 2018 received more precipitation than all of the year’s December months combined. The years 2019 to 2021 received some variations.

There will be no correlation in the precipitation values among the years as shown in Figure 27.

**Table 3.** Analysis for the month of December (2015-2021)

Year	Precipitation	Runoff
Dec-21	12.456	1.044
Dec-20	30.623	12.288
Dec-19	24.722	10.084
Dec-18	49.914	6.22
Dec-17	8.932	1.006
Dec-16	34.78	12.625
Dec-15	18.352	8.434



**Figure 27.** Analysis for the month of December (2015-2021)

As shown in Figure 28, January has seen a slow upgrade in precipitation and runoff values from 2015 to 2017, but there is an abrupt change in January 2018. This month received more rainfall when compared to January 2017. There is a correlation between January 2018 and January 2021.

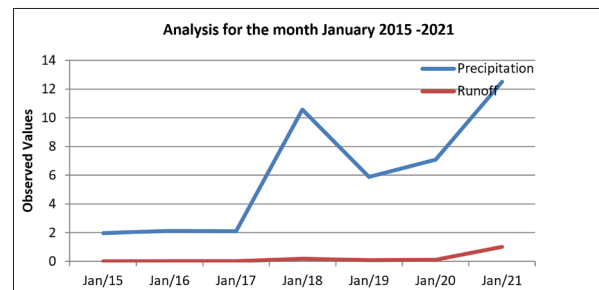


**Figure 28.** Analysis for January (2015-2021)

Table 4 shows the complete precipitation and runoff analysis for January from 2015 to 2021. Since 2018, every year has received more precipitation and higher runoff values than the previous years. The January of 2021 received the highest rainfall (12 mm); there was very little rainfall in December 2021 compared to previous years. It shows that there are more variations in the rainfall rate every year and that slow developments in climate change are happening in Andhra Pradesh.

**Table 4.** Analysis for the month of January (2015-2021)

Year	Precipitation	Runoff
Jan-21	12.508	1.008
Jan-20	7.1	0.106
Jan-19	5.888	0.082
Jan-18	10.567	0.189
Jan-17	2.094	0.02
Jan-16	2.121	0.021
Jan-15	1.963	0.016



- RS and GIS-based SCS-CN method. *Water*, 12(7), 1–16. <https://doi.org/10.3390/w12071924>
- Anderson, Z., Chen, Q., Kavvas, M. L., & Feldman, A. (2004). Coupling HEC-HMS with atmospheric models for the prediction of watershed runoff. In *Joint Conference on Water Resources Engineering and Water Resources Planning and Management 2000 Building Partnerships* (pp. 312–318). [https://doi.org/10.1061/40517\(2000\)135](https://doi.org/10.1061/40517(2000)135)
- Animashaun, P. G., Oguntunde, A. S., Akinwumiju, A. S., & Olubanjo, O. O. (2020). Rainfall analysis over the Niger central hydrological area, Nigeria: Variability, trend, and change point detection. *Scientific African*, 8, e00419. <https://doi.org/10.1016/j.sciaf.2020.e00419>
- Arnold, J. G., & Allen, P. M. (1996). Estimating hydrologic budgets for three Illinois watersheds. *Journal of Hydrology*, 176(1–4), 57–77. [https://doi.org/10.1016/0022-1694\(95\)02782-3](https://doi.org/10.1016/0022-1694(95)02782-3)
- Arvind, P., Ashok Kumar, S., Girish Karthi, S., & Suribabu, C. R. (2017). Statistical analysis of 30 years rainfall data: A case study. In *IOP Conference Series: Earth and Environmental Science* (Vol. 80, No. 1). <https://doi.org/10.1088/1755-1315/80/1/012067>
- Attah, U. E., Joshua, O. I., & Emmanuel, O. (2020). Susceptibility of agricultural land to soil degradation by rainfall using aggregates' stability indices in parts of Abia State, South Eastern Nigeria. *Jordan Journal of Earth and Environmental Sciences*, 11(4), 211.
- Baquero, S., Cruz-Pol, S., Bringi, V. N., & Chandrasekar, V. (2005). Rain-rate estimate algorithm evaluation and rainfall characterization in tropical environments using 2DVD, rain gauges, and TRMM data. In *International Geoscience and Remote Sensing Symposium* (Vol. 2, pp. 1146–1149). <https://doi.org/10.1109/IGARSS.2005.1525319>
- Chormanski, J., Van de Voorde, T., De Roeck, T., Batelaan, O., & Canters, F. (2008). Improving distributed runoff prediction in urbanized catchments with remote sensing-based estimates of impervious surface cover. *Sensors*, 8(2), 910–932. <https://doi.org/10.3390/s8020910>
- Ebrahimiyan, L., See, L. F., Ismail, M. H., & Malek, I. A. (2009). Application of natural resources conservation service curve number method for runoff estimation with GIS in the Kardeh watershed, Iran. *European Journal of Scientific Research*, 34(4), 575–590.
- Eliza, H., Mohamad, W. Y., & Yusop, Z. (2016). Rainfall analysis of the Kelantan big flood. *Jurnal Teknologi*, 4, 83–90.
- Fowler, K., Peel, M., Saft, M., Peterson, T. J., Western, A., Band, L., & Nathan, R. (2022). Explaining changes in rainfall-runoff relationships during and after Australia's Millennium Drought: A community perspective. *Hydrology and Earth System Sciences Discussions*, in review. <https://doi.org/10.5194/hess-2022-147>
- Gupta, N., & Dixit, J. (2022). Estimation of rainfall-induced surface runoff for the Assam region, India, using the GIS-based NRCS-CN method. *Journal of Maps*. <https://doi.org/10.1080/17445647.2022.2076624>
- Gholami, V., & Khaleghi, M. R. (2021). A simulation of the rainfall-runoff process using artificial neural network and HEC-HMS model in forest lands. *Journal of Forest Science*, 67(4), 165–174. <https://doi.org/10.17221/90/2020-JFS>
- Hassan, G. A., Isaac, P. A., Taylor, P. A., & Michelson, D. (2022). Optimizing radar-based rainfall estimation using machine learning models. *Remote Sensing*, 14(20). <https://doi.org/10.3390/rs14205188>
- Jehanzaib, M., Ajmal, M., Achite, M., & Kim, T. W. (2022). Comprehensive review: Advancements in rainfall-runoff modelling for flood mitigation. *Climate*, 10(10), 1–17. <https://doi.org/10.3390/cli10100147>
- Ling, Z., Yusop, Z., Yap, W. S., Tan, W. L., Chow, M. F., & Ling, J. L. (2020). A calibrated, watershed-specific SCS-CN method: Application to Wangjiaqiao watershed in the Three Gorges area, China. *Water*, 12(1). <https://doi.org/10.3390/w12010060>
- Liu, H., Zhou, D., Li, D., Zeng, L., & Xu, P. (2023). Evaluation of artificial precipitation enhancement using UNET-GRU algorithm for rainfall estimation. *Water*, 15(8). <https://doi.org/10.3390/w15081585>
- Loveridge, F., & Rahman, A. (2021). Effects of probability-distributed losses on flood estimates using event-based rainfall-runoff models. *Water*, 13(15), 1–18. <https://doi.org/10.3390/w13152049>
- Mohammadi, M. J., Safari, S., & Vazifehkhah, S. (2022). IHACRES, GR4J and MISD-based multi conceptual-machine learning approach for rainfall-runoff modeling. *Scientific Reports*, 12(1), 1–21. <https://doi.org/10.1038/s41598-022-16215-1>
- Moglen, G. E., Sadeq, H., Hughes, L. H., Meadows, M. E., Miller, J. J., Ramirez-Avila, J. J., & Tollner, E. W. (2022). NRCS curve number method: Comparison of methods for estimating the curve number from rainfall-runoff data. *Journal of Hydrologic Engineering*, 27(10), 1–10. [https://doi.org/10.1061/\(ASCE\)HE.1943-5584.0002210](https://doi.org/10.1061/(ASCE)HE.1943-5584.0002210)
- Musgrave, G. W. (1955). How much of the rain enters the soil? *Yearbook of Agriculture*, 1951–1960.
- Nganro, S., Trisutomo, R. A., Barkey, M., & Ali, M. (2020). Rainfall analysis of the Makassar city using Thiessen polygon method based on GIS. *Journal of Engineering and Applied Sciences*, 15(6), 1426–1430. <https://doi.org/10.36478/jeasci.2020.1426.1430>
- Psomiadis, K., Soulis, X., Zoka, M., & Dercas, N. (2019). Synergistic approach of remote sensing and GIS techniques for flash-flood monitoring and damage assessment in Thessaly plain area, Greece. *Water*, 11(3). <https://doi.org/10.3390/w11030448>
- Psomiadis, K., Soulis, X., & Efthimiou, N. (2020). Using SCS-CN and Earth observation for the comparative assessment of the hydrological effect of gradual and abrupt spatiotemporal land cover changes. *Water*, 12(5). <https://doi.org/10.3390/w12051386>
- Rajbanshi, R. (2016). Estimation of runoff depth and volume using NRCS-CN method in Konar catchment (Jharkhand, India). *Journal of Civil and Environmental Engineering*, 6(4), 4–9. <https://doi.org/10.4172/2165-784x.1000236>
- Raza, A., et al. (2023). Water resources and irrigation management using GIS and remote sensing techniques: Case of Multan district (Pakistan). In C. B. Pande, M. Kumar, & N. L. Kushwaha (Eds.), *Surface and groundwater resources development and management in semi-arid region*. Springer Hydrogeology. Springer, Cham. [https://doi.org/10.1007/978-3-031-29394-8\\_8](https://doi.org/10.1007/978-3-031-29394-8_8)
- Salahat, M. A., & Al-Qinna, M. I. (2015). Rainfall fluctuation for exploring desertification and climate change: New aridity classification. *Jordan Journal of Earth and Environmental Sciences*, 7(1), 27–35.
- Saragih, N. F., Sitepu, S., Simanungkalit, G. T., Sinambela, M., Rajagukguk, E., Larosa, F. G., & Jaya, I. K. (2022). Validation of CHIRPS estimation rainfall data using numerical accuracy test with precipitation observation data. In *IOP Conference Series: Earth and Environmental Science* (Vol. 1083, No. 1). <https://doi.org/10.1088/1755-1315/1083/1/012095>
- Sayd, D., Yonnana, E., & Mubi, A. (2020). An analysis of rainfall and discharge relationship at the River Kilange catchment, Adamawa State, Nigeria. *Jordan Journal of Earth and Environmental Sciences*, 11(4).
- Seong, C., Choi, K., & Jung, Y. (2022). Assessment of uncertainty in grid-based rainfall-runoff model based on

- formal and informal likelihood measures. *Water*, 14(14). <https://doi.org/10.3390/w14142210>
- Sishah, M. (2021). Rainfall runoff estimation using GIS and SCS-CN method for Awash river basin, Ethiopia. *International Journal of Hydrology*, 5(1), 33–37. <https://doi.org/10.15406/ijh.2021.05.00263>
- Soulis, X., & Dercas, N. (2007). Development of a GIS-based spatially distributed continuous hydrological model and its first application. *Water International*, 32(1), 177–192. <https://doi.org/10.1080/02508060708691974>
- Soulis, X., & Valiantzas, J. D. (2012). SCS-CN parameter determination using rainfall-runoff data in heterogeneous watersheds-the two-CN system approach. *Hydrology and Earth System Sciences*, 16(3), 1001–1015. <https://doi.org/10.5194/hess-16-1001-2012>
- Soulis, X., Valiantzas, J. D., Dercas, N., & Londra, P. A. (2009). Analysis of the runoff generation mechanism for the investigation of the SCS-CN method applicability to a partial area experimental watershed. *Soil Conservation*, 605–615.
- Verma, R. K., Verma, S. K., Mishra, A., Singh, A., & Jayaraj, G. K. (2017). A revisit of NRCS-CN inspired models coupled with RS and GIS for runoff estimation. *Hydrological Sciences Journal*, 62(12), 1891–1930. <https://doi.org/10.1080/02626667.2017.1334166>
- Wei, Y., Yu, J., Xiao, J., & Chen, L. (2018). Rainfall-runoff risk characteristics of urban function zones in Beijing using the SCS-CN model. *Journal of Geographical Sciences*, 28(5), 656–668. <https://doi.org/10.1007/s11442-018-1497-6>
- Wetchayont, C., Ekkawatpanit, S., Rueangrit, S., & Manduang, J. (2023). Improvements in rainfall estimation over Bangkok, Thailand, by merging satellite, radar, and gauge rainfall datasets with the geostatistical method. *Big Earth Data*, 1–25. <https://doi.org/10.1080/20964471.2023.2171581>
- Zhang, F. (2019). Application of NRCS-CN method for estimation of watershed runoff and disaster risk. *Geomatics, Natural Hazards and Risk*, 10(1), 2220–2238. <https://doi.org/10.1080/19475705.2019.1686431>
- Zhang, W., Fang, X., Jia, X., & Sheng, V. S. (2022). Research on rainfall estimation based on improved Kalman filter algorithm. *Journal of Quantum Computing*, 4(1), 23–37. <https://doi.org/10.32604/jqc.2022.026975>
- Zhang, N., Wang, S., & Luo, L. (2011). Initial abstraction ratio in the SCS-CN method in the Loess Plateau of China. *Transactions of the ASABE*, 54(1), 163–169. <https://doi.org/10.13031/2013.36271>